***Graphical Abstract**

Graphical abstract

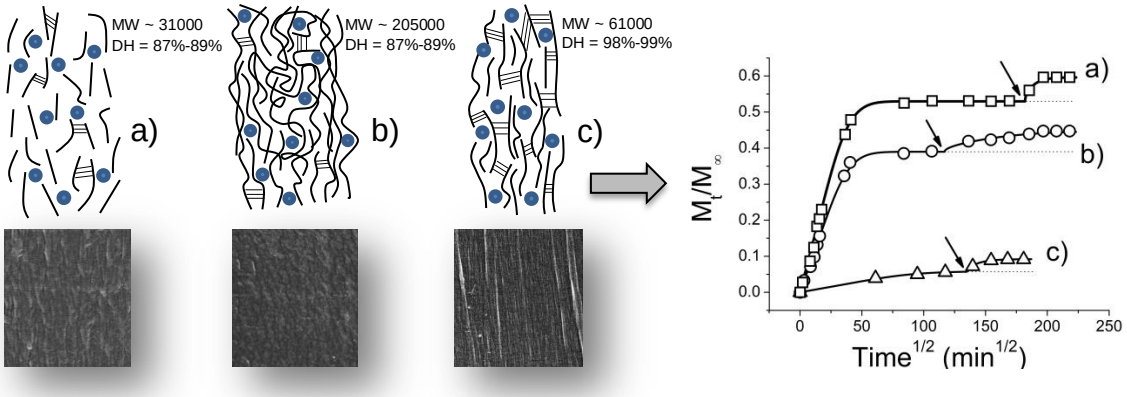

Research Highlights

- The release of a dye from PVOH films in hydro-alcoholic medium was described
- Physicochemical differences of the polymer matrix influenced the release kinetics
- Molecular weight and degree of hydrolysis played a key role on the release properties
- Due to its non-solvent behavior, ethanol hindered the release process
- Tailored controlled release patterns were achieved

Dye release behavior from polyvinyl alcohol films in a hydro-alcoholic medium: influence of physicochemical heterogeneity

Carlo A. Cozzolino[a,c], Thomas O. J. Blomfeldt[b], Fritjof Nilsson[b], Antonio Piga[a], Luciano Piergiovanni[b], Stefano Farris[b,c*]

[a]DiSAABA, Department of Agricultural Environmental Science and Agri-Food Biotechnology, – University of Sassari, Viale Italia 39/A, 07100 Sassari, Italy

[b]Department of Fiber and Polymer Technology, KTH Royal Institute of Technology, SE-10044, Stockholm, Sweden

[c]DiSTAM, Department of Food Science and Microbiology, Packaging Division – University of Milan, Via Celoria 2 - 20133 Milan, Italy

*Corresponding author. Tel.: +39 0250316654; fax: +39 0250316672

E-mail address: stefano.farris@unimi.it (S. Farris).

Abstract

In this paper we investigated the release kinetics of a model drug-like compound (Coomassie brilliant blue) from polyvinyl alcohol (PVOH) films into a hydro-alcoholic solution as a function of the physicochemical properties of the polymer matrix. After 33 days of monitoring, the total amount released ranged from 10% for the high hydrolysis degree/low molecular weight PVOH films to 60% for the low hydrolysis degree/low molecular weight films. Mathematical modeling allowed for an estimation of the two diffusion coefficients (D_1 and D_2) that characterized the release profile of the dye from the films. The degree of hydrolysis dramatically affected both the morphology and the physical structure of the polymer network. A high hydroxyl group content was also associated with the shifting of second order and first order transitions towards higher temperatures, with a concurrent increase in crystallinity. Moreover, the higher the degree of hydrolysis, the higher the affinity of the polymer to the negatively charged molecule dye. Selection of the polymer matrix based on physicochemical criteria may help in achieving different release patterns, thereby representing the first step for the production of polymer systems with modulated release properties.

Keywords: controlled release; diffusion; modeling; morphology; polyvinyl alcohol

1. Introduction

Polyvinyl alcohol (PVOH) is an attractive polymer for many different applications. It has been widely used in many fields, such as: environmental, for the production of films for the removal of heavy metal ions in water [1]; pharmaceutical, for the obtainment of wound-dressing systems [2] and biomedical, as a scaffold supporting material for tissue engineering applications [3]. Other applications include agriculture [4], packaging [5], fuel cells [6], and electrochemistry [7]. In addition, PVOH is well suited both to produce electrospun nanofibrous mats [8] and to develop polymer blends in association with many biopolymers [10–13]. The success of PVOH is due to many reasons, first of all because of its unique molecular structure and properties, such as its rubbery or elastic nature and its high degree of swelling in aqueous solutions [14]. Moreover, the hydroxyl pendant group on every second carbon atom on its backbone allows PVOH to take part in many chemical cross-linking reactions [15], interact with many other polymers, primarily through hydrogen bonding [16], and form a physical hydrogel through the well-known freeze-thaw process [17]. Inherent non-toxicity, non-carcinogenicity, and good biocompatibility represent additional desirable features. Finally, PVOH is the only known purely C–C macromolecule that can be biodegraded [18].

One of the main interests in PVOH-based polymer systems lies in the development of smart devices with tunable release properties. In this respect, long established fields of application are the pharmaceutical and biomedical industries, where PVOH has been extensively used as a privileged polymer for the encapsulation/loading and the subsequent release of enzymes [19], proteins [20], cells [21] and, more broadly, a huge variety of drugs [22–25]. However, the field of sustained delivery of active compounds is advancing rapidly, and new applications within sectors that traditionally lagged behind the aforementioned established fields came about during the last decades.

Among others, novel release systems are expected to grow in the coming years within the food packaging field, due to the increasing interest towards the concept of active packaging [26]. The

underlying basic idea is to convey an active molecule (e.g. anitimicrobial, antioxidant, etc.) from the polymeric reservoir to the target body (i.e. the food), maintaining its concentration to a predetermined level over a required time span. This can be accomplished if the polymer system 'senses' and 'responds' to specific stimuli, such as temperature [27], surrounding medium [28], pH [22,29], light [30], ultrasound [31], electric field [23,32], etc., which act as triggers. The main relevant advantage of this approach is that it allows avoidance of either multiple supplies or direct addition of a large amount of the active compound directly into the target body. However, to make release systems work efficiently, controlling the delivery rate over time in a deliberate manner is the crucial point. This is why 'controlled release system' (CRS) appears in most cases a more appropriate definition. In light of these considerations, both the comprehension of the phenomena underlying the release process and the description of the release kinetics through mathematical models appear necessary steps for the design and development of any controlled delivery device.

In this work, we investigated the release properties of PVOH films as a function of physicochemical aspects such as degree of hydrolysis (DH) and molecular weight (MW), which have been indicated as the two most important parameters influencing the release performance of the polymer matrix [33]. In addition, a mechanistic approach was adopted to properly describe the release kinetics through a specific mathematical model. Despite the fact that many studies have been published on the release from PVOH matrices, all of them referred to the release from a hydrophilic polymer (i.e. the PVOH) to a hydrophilic medium (usually water). In this respect, the release kinetic from polyvinylalchol into aqueous solution is primarily driven by the swelling of the polymer matrix [34,35]. Conversely, no detailed works on the release kinetics from PVOH matrices in contact with a hydro-alcoholic liquid medium have been retrieved in the literature. For this reason, in this work we used a hydro-alcoholic solution as the delivery medium. This choice also accounts for the fact that hydro-alcoholic media are often encountered in the everyday life (e.g. food, drinks, cosmetics, and health care

products). Moreover, water/ethanol solutions are food simulants within the food contact material legislation [36]. The interest in elucidating the release behavior of PVOH films in hydro-alcoholic environments is thus manifold. An anionic low molecular weight dye was used as the model drug-like compound due to its similarity to many small molecules used in sustained delivery applications [37].

2. Experimental

2.1. Materials

Three different types of polyvinyl alcohol (Fluka Analytical, Milan, Italy) in the form of pellets were used in this work: 1) PVOH 4-88, with DH 86.7-88.7 mol%; MW ~31000; viscosity (4% aqueous solution at 20°C) 3.5–4.5 mPa s; degree of polymerization ~630; ester number 130-150; 2) PVOH 40-88, with DH 86.7-88.7 mol%; MW ~205000; viscosity (4% aqueous solution at 20°C) 38–42 mPa s; degree of polymerization ~4200; ester number 130-150; 3) PVOH 10-98, with DH 98.0-98.8 mol%; MW ~61000; viscosity (4% aqueous solution at 20°C) 9–11 mPa s; degree of polymerization ~1400; ester number 15-25. Coomassie Brilliant Blue G-250 (sodium 3-[[4-[(E)-[4-(4-ethoxyanilino)phenyl]-[4-[ethyl-[(3-sulfonatophenyl)methyl]azaniumylidene]-2-methylcyclohexa-2,5-dien-1-ylidene]methyl]-N-ethyl-3-methylanilino]methyl]benzenesulfonate; molecular weight = 854.02 Da; maximum absorbance λ_{max} = 610 nm) – Sigma Aldrich, Milan, Italy), was used as the model active compound. Milli-Q water (18.3 MΩ cm) and ethanol (purity ≥ 99.8%, Fluka Analytical, Milan, Italy) were used for the preparation of the hydro-alcoholic polymer-dye solutions.

2.2. Film preparation

The PVOH water solutions were prepared by dissolving 5 g of PVOH in 95 mL of hot water (92°C) for 1 h under gentle stirring (500 rpm). After cooling at room temperature, the film-forming solutions (pH = 5.5 ± 0.1) were loaded with the dye powder (0.052% weight of dye/weight of dry

polymer), which dissolved rapidly under gentle stirring. At this pH, the dye molecules carry a net negative charge [38] (Figure 1).

Next, 5 g of the obtained solutions were poured on glass Petri plates (6 cm in diameter) and dried in an oven at 55°C for 24 h. Dried films (surface area of 28.27 cm^2 with an average thickness of 61.4 ± 0.7 μm) were then peeled off the plate and, before analyses, stored for 2 weeks in a desiccator containing silica gel. Residual moisture of the coatings after drying was measured by means of a halogen moisture analyzer, mod. HG63 (Mettler Toledo, Zurich, Switzerland). The thickness of the dry films was measured using a micrometer (Dialmatic DDI030M, Bowers Metrology, Bradford, UK) to the nearest 0.001 mm at 10 different random locations. Unless otherwise specified, all data shown are the average of five replicates.

2.3. Dye release kinetics

Dye-loaded PVOH films were put into flasks containing 50 mL of a hydro-alcoholic solution (water/ethanol = 1/9) as the releasing medium. This mixture allowed monitoring of the dye release over an extended temporal window without dissolution of the physically cross-linked PVOH network, owing to the non-solvent feature of ethanol towards this polymer [39]. The dye release experiments were conducted by keeping the flasks at 20°C under moderate shaking (100 rpm) using a Flask Dancer 270292 orbital shaker from Boekel Scientific (Feasterville, PA, USA). The dye release kinetics were built by assessing the dye concentration in the hydro-alcoholic solution over a time span of 47700 minutes (i.e. ~ 33 days). Absorption of the dye at 610 nm was recorded at different time intervals using a Lambda 650 UV/VIS spectrophotometer (PerkinElmer, Waltham, MA, USA). The absorbance values were then converted into concentration values by the calibration curve, which was obtained by means of standard solutions (three replicates) from 1 ppm to 100 ppm (mg / kg). Each data point of the release curves represents the mean of nine replicates.

The swelling ratio (*SR*) was calculated on a second set of PVOH films according to the following formula:

$$SR(\%) = \frac{W_w - W_d}{W_d} \times 100 \quad (1)$$

where W_w and W_d are the wet and dry weight (g) of the PVOH films, respectively. Since it was not possible to handle the samples 4-88 and 40-88 after 13 days soaking in the water/ethanol solutions, swelling evolution was no longer monitored after 13 days.

2.4. X-ray diffraction (XRD)

The X-ray diffraction patterns of the films were obtained using a Rigaku DMAX-II diffractometer (Rigaku Corporation, Tokyo, Japan) with graphite-monochromatized Cu-Kα radiation (1.5406 Å) and a generator operating at 40 kV and 40 mA, under the following conditions: step width 0.02°; time per step 2 s; divergence slit 1.0 °; soller slit 1.0 °; antiscatter slit 0.15 °.

2.5. Differential Scanning Calorimetry (DSC)

The thermal properties of the PVOH samples were determined by differential scanning calorimetry (DSC) analysis using a DSC 1 (Mettler Toledo, Columbus, OH) supplied with a quench-cooling accessory and a GC 100 gas controller. Before measurements, the instrument was calibrated with the well-characterized standard indium, which has a heat of fusion (ΔH) of 28.4 J/g and a melting temperature (T_m) of 156.6°C. Approximately 5 mg PVOH samples were then put in a hermetically sealed aluminum pan (40 μL) to prevent any loss of moisture during the experiment. An initial scan from 25°C to 250°C was followed by an isothermal step (250°C for 5 min), with the goal of better determining the crystallization temperature. Samples were then cooled to 25°C. The second heating scan was carried out from 25°C to 250°C. All scans were performed in an inert environment (50 mL

min^{-1} N_2) at a rate of 10°C min^{-1}. The glass transition temperature (T_g) was calculated as the midpoint of the inflexion in the baseline (second heating scan) caused by the discontinuity of the specific heat capacity of the sample. The melting temperature (T_m) was set at the endothermic peak, which was also used to calculate the degree of crystallinity according to the following formula, assuming a linear relationship between the peak area and crystallinity [40]:

$$x_c(\%) = \frac{\Delta H}{\Delta H_{100}} \cdot 100 \quad (2)$$

where X_c is the crystallinity of the semi-crystalline polymer, ΔH the experimental heat of fusion (J g^{-1}) and ΔH_{100} the heat of fusion of the 100% crystalline material (equal to 138.6 J g^{-1} for PVOH). All the above parameters were calculated by the software Star^e version 9.20 (Mettler Toledo, Columbus, OH, USA). Three replicates were used for each of the three PVOH films.

2.6. Field-Emission Scanning Electron Microscopy (FE-SEM)

Cross-sections and surfaces of PVOH films were examined using a Hitachi S-4800 FE-SEM (Schaumburg, IL, USA) in order to acquire information on the overall physical organization of the polymer network. Surface test specimens were mounted with carbon tape on stubs. Cross-sectioned samples were cut into thin pieces with a scalpel and mounted on a Hitachi thin specimen split mount holder, M4 (prod. No 15335-4) to observe the cross-section. Before insertion into the microscope, samples were sputter coated with gold to a thickness of approximately 10 nm (to avoid charging the samples), using an Agar High Resolution Sputter Coater (model 208RH), equipped with a gold target/Agar thickness monitor controller.

2.7. Statistical Analysis

Statgraphics Plus 4.0 software (STSC, Rockville, USA) was used for the one-way ANOVA to check for differences between samples. The mean values, when appropriate, were separated by the LSD multiple range test at $p < 0.05$. The dye kinetic release curves were obtained by fitting the analytical solution of Fick's second law for a planar sheet to the experimental data solved using Matlab® (The Mathworks Inc., Natick, MA, USA).

3. Results and discussion

3.1. Dye release kinetics

The ethanol-rich solvent mixture used in this work made it possible to preserve the integrity of the PVOH films over 33 days of monitoring; no secondary effect (e.g. dissolution, crazing, wrinkling, or breakage) besides swelling occurred macroscopically on the PVOH samples during the release experiments. Therefore, it can be reasonably assumed that the release took place from a planar sheet throughout the entire time span of analysis. Generally, the overall release process of low molecular weight compounds from strongly hydrophylic networks (such as PVOH) can be conceived as the result of three phenomena: i) solvent diffusion into the film network; ii) relaxation of the polymer matrix, owing to the swelling of the strongly hydrophilic PVOH molecules; iii) diffusion of the active compound from the swollen polymeric network into the surrounding medium. Due to both the complexity of simultaneous monitoring of the abovementioned phenomena and the presence of ethanol, it has been demonstrated as expedient to model the experimental release data by a simple approach under the following assumptions [41]: 1) both water diffusion and relaxation of molecular chains are faster than the diffusion of the low molecular weight compound through the slightly swollen network, 2) the increase in film size due to swelling is negligible, and 3) dye diffusion takes place in an homogeneous and symmetric medium. Moreover, the volume of the liquid medium has been

considered infinite and it has been assumed that the external mass transfer coefficient at the solid-liquid interface is negligible. The solution of Fick's second law for a planar sheet with constant boundary conditions can thus be used [42]:

$$M_t = M_\infty \left\{ 1 - \frac{8}{\pi^2} \sum_{n=0}^{n=\infty} \frac{1}{(2n+1)^2} \exp\left[-\frac{D_{dye}}{l^2} (2n+1)^2 \pi^2 t \right] \right\} \quad (3)$$

where M_t represents the amount (mg/kg) of the diffusing compound released at time t (s); M_∞ is the corresponding amount at infinite time (i.e. at the equilibrium), taken as the initial quantity loaded in the film; D_{dye} is the dye apparent diffusion coefficient (cm^2/s) through the polymeric matrix, l is the thickness (cm) of dry films. The release kinetics were obtained plotting the M_t / M_∞ ratio versus the square root of time, in order to elucidate the diffusion behavior of the low molecular weight molecule according to the classification proposed by Crank [43].

Figure 2a displays the experimental release data. The final amount of dye released from samples 4-88, 40-88, and 10-98 after 33 days accounted for, respectively, 60%, 45%, and 10% of the initial amount loaded in the films. Besides physicochemical considerations, which will be discussed shortly, newly established weak interactions (e.g., ion-dipole forces) between the negatively charged dye and the polar pendant hydroxyl groups along the PVOH backbone could have contributed in thwarting the diffusion process of the small molecule dye. Although this conclusion cannot be directly induced from our data, the different affinity of the dye for the polymer matrix can be deduced by the partition coefficients calculated for each film at infinite time according to the following formula:

$$K = \frac{C_{polymer,\infty}}{C_{solvent,\infty}} \quad (4)$$

where $C_{polymer,\infty}$ and $C_{solvent,\infty}$ are, respectively, the migrant concentration (mg/kg) in the polymer and in the liquid medium at the equilibrium. The resulting K values are reported in Table 1. Since this coefficient compares the relative affinity of the migrant between polymer and solvent, the following

classification accounting for the affinity of the three PVOH films for the dye can be gathered: 10-98 > 40-88 > 4-88, which confirms the previous hypothesis of an increased number of interactions for the –OH richest PVOH films.

Another striking feature is that all samples showed an initial "induction" or "lag" phase, here intended as the time required before the release process set off (see the inset of Figure 2a). A plausible explanation for the appearance of such 'no-release' lapse can be the simultaneous presence of both a non-solvent (ethanol) and a solvent (water) in contact with the polymer matrix. Water-ethanol interactions modify the availability of water molecules towards the polymer matrix, thus slowing down the relaxation of the polymer chains [44]. This is also confirmed by the swelling ratio values collected during the induction phase (Figure 3a). These values are noticeably lower than those otherwise obtained from uncross-linked and cross-linked PVOH samples immersed in a 100% water solution at room temperature during a time span of similar magnitude [35].

Figure 2b displays the fitting of the mathematical model expressed by equation 3 to the experimental data. This procedure allowed for estimating the apparent diffusion coefficient (D) of the released dye molecules for all three PVOH films. Due to the hypotheses made for deriving equation 3, D has to be considered with any thermodynamic meaning. For this reason, it can be more useful to consider the ratio D/l^2 since it is directly related to the dye release rate from the film to the outer hydro-alcoholic solution [41]. The D_1/l^2 values can be easily inferred from Table 1. This ratio was greatly decreased for sample 10-98 (3.68×10^{-7} s^{-1}) compared to samples 40-88 (2.02×10^{-6} s^{-1}) and 4-88 (2.05×10^{-6} s^{-1}). Equation 3 was also fit to the experimental data underlying the sudden jump observable in the dye release evolution (see arrow in Figure 2b). The appearance of the film burst, already reported for PVOH-based release systems [44], can be reasonably attributed to the partial collapse of the amorphous phase, which ultimately produced an increase in the total amount of the dye molecule released into the surrounding medium. It was possible to associate a second diffusion coefficient (D_2)

for all the three PVOH samples (Table 1) by a new independent procedure that took into account new and different starting points (t_1, t_2, and t_3 for PVOH samples 40-88, 10-98, and 4-88, respectively, see Figure 2b). The D_2/l^2 values were significantly lower for sample 40-88 (1.42×10^{-7} s^{-1}) compared to samples 10-98 and 4-88 (6.31×10^{-7} s^{-1} and 6.15×10^{-7} s^{-1}, respectively), presumably due to the higher molecular weight, i.e. higher degree of molecular chain entanglement.

Eventually, the three PVOH samples, although released a different amount of dye as clearly depicted in Figure 2c, had in common a similar release profile characterized by a lag-phase followed by a first rapid release step and a second release burst. As anticipated, the release patterns disclosed by the PVOH films will be now discussed on the basis of physical aspects intimately linked to the chemical structure of the three PVOH matrices.

3.2. XRD analysis

Figure 4 shows the XRD patterns for the three different PVOH films tested in this work, while the main parameters drawn from the diffractograms are reported in Table 2. All the three samples exhibited one strong peak at $2\theta \sim 19°$ and a second weaker peak at $2\theta \sim 40.5°$. The latter has been attributed to the (2 2 0) reflection [45], whereas the former peak has been already reported to correspond to a typical doublet reflection of (1 0 1) and (1 0−1) planes of the semicrystalline atactic PVOH containing the extended planar zigzag chain conformation [46,47]. However, this peak was gradually shifted to lower diffraction angles from sample 4-88 to sample 10-98, with sample 40-88 in between. Shifting towards lower angles is generally correlated to an increase in periodicity of the crystalline structure, implying an increase in the size of the PVOH crystallites [46], in agreement with the results obtained by applying the Scherrer equation for the estimation of the size (thickness, $\overline{D}_{hkl}$) of the crystallites:

$$\overline{D}_{hkl} = \frac{K\lambda}{\beta \cos\theta} \quad (5)$$

where K is the Scherrer shape factor near unity (here set at the value of 0.94), λ is the wavelength of the X-ray, β is the breadth (in radians, at half the peak value) of the diffraction peak associated with the (*hkl*) planes, and θ the diffraction angle (in radians) [48]. Data on the crystallite dimensions, reported in Table 2, are indicative of the fact that the crystallite domains in sample 10-98 were larger compared to those in samples 40-88 and 4-88, the latter sample apparently having the smallest crystallite size. Concurrently, the diffraction peak related to sample 10-98 became narrower and sharper compared to the other two peaks, suggesting more closely packed crystallites with fewer imperfections [17,49].

According to the release data illustrated in the previous section, both the degree of crystallinity and the crystal organization apparently played an important role in the diffusion kinetics of the dye molecules into the hydro-alcoholic medium. The different degree of crystallinity seems to justify the extended induction phase observed for the sample 10-98 (~ 8 days compared to ~ 1.5 h and ~ 2 h for samples 4-88 and 40-88, respectively), as the higher amount of crystallite regions could have induced a decrease in the relaxation rate of the polymer chains (the only phase available for water uptake is the amorphous one). Therefore, the presence of the crystal phase in the film would have a similar effect as chemical crosslinking in amorphous polymers [50]. In addition, the total release of dye decreased proportionally to the degree of crystallinity, most likely due to the physical impedance offered by the crystal regions to the diffusion of the dye. The D_1/l^2 values calculated for the three PVOH films are consistent with the generally accepted rule that D decreases with an increase in crystallinity, basically due to an increase in both the tortuosity factor (linked to the physical obstacles represented by the crystallite regions) and the chain-immobilization factor (linked to the restriction of chain movement in the amorphous phase). We also believe that part of the dye loaded in the PVOH water solutions got entrapped during the formation of the crystalline domains (i.e. during the drying process) and there was retained throughout the release experiment duration, as suggested by the total amount of the dye released after 33 days, which never reached the theoretical 100%. According to this hypothesis, the

work of Mallapragada and Peppas [51] demonstrated that the drug release from semicrystalline polymers physically crosslinked (such as the PVOH films used in this work) is controlled by the rate of crystals dissolution in a solvent, i.e. the total release could never be achieved as long as the crystal phase is not completely dissolved.

This observation indicates that the crystalline phase of the PVOH films used in this work was not dissolved upon contact with the hydro-alcoholic medium. This was also corroborated by the swelling ratio data. Samples soaked in the hydro-alcoholic medium never experienced abrupt volumetric expansion, and the swelling ratio values after 13 days (Figure 3b) were well below the range 200%–500% observed for both PVOH films of different DH immersed in pure water [44] and PVOH films immersed in several mixed solvents of dimethylsulfoxide (DMSO) and water with different solvent compositions [50] after the same time span. In addition, samples 10-98, 40-88 and 4-88 did not dissolve in the medium after 33 days, while the same samples in direct contact with pure water dissolved completely, as demonstrated by our preliminary experiments (data not shown). This is in agreement with previous results that suggest the complete disruption of the crystalline domains of untreated PVOH films, i.e. subjected to neither annealing [47] nor freezing-thawing [52]. Since the polymer will not dissolve until the crystal structure is broken down [47], the original crystalline pattern of the three PVOH samples is thought to have not been greatly affected by the water molecules. This was also demonstrated by Sakurada et al. [53], who analyzed the crystallinity of swollen PVOH films, showing that swelling does not change (‘melt out’) the crystalline regions of the PVOH matrix. However, it has been pointed out that the average size of the crystallite, its size distribution and the packing order of molecules in crystallites are variable factors within the total crystallinity and some of the smaller crystals or with a lower degree of packing order might have experienced partial dissolution on swelling [50]. Therefore, based on the above considerations, while we can assume with a degree of certainty that the crystallinity (x_c) of sample 10-98 did not change significantly after contact with the

water/ethanol medium, the x_c values of samples 40-88 and 4-88 might have slightly decreased during swelling.

3.3. DSC analysis

DSC traces (Figure 5) display the differences between the samples as far as their thermal properties are concerned. The thermal parameters drawn from the DSC analysis are summarized in Table 3. The difference in T_g between sample 4-88 and sample 40-88 can be explained by Flory's theory, according to which the glass transition temperature decreases with decreasing molecular weight due to an increased segmental mobility of the polymer chains [54]. The highest T_g observed for sample 10-98 accounts for the high packing efficiency of the planar zigzag conformation [55]. The effect of the crystal phase on the mobility of the amorphous molecules must also be mentioned, since the tension of the amorphous molecules should be enhanced by the formation of the crystallites [50]. The melting temperatures recorded reflected the capability of the polymer chains to arrange into ordered domains. This is believed to be enhanced by the small size of the hydroxyl groups, which allows the chains to adopt a planar zigzag conformation under the action of hydrogen bonding between the pendant hydroxyl groups along the molecule [56,57]. Although no statistically significant difference was detected between samples 4-88 and 40-88 concerning the T_m, the former sample showed a higher tendency to form crystal regions, which was also confirmed by the observed trend in the degree of crystallinity. Presumably, this might be due to the higher molecular weight of sample 40-88, which could have hindered the re-organization of the molecular chains into ordered domains upon cooling, thus favoring the growth of the amorphous phase. This was also confirmed by the swelling ratio evolution reported in Figure 3a: the higher solvent uptake by sample 40-88 during the first 24 hours could be linked to a larger amorphous phase compared to sample 4-88. Both T_m and crystallinity increased dramatically for sample 10-98, in line with the values reported in the literature for highly

hydrolyzed atactic PVOH polymers [46,50] and in agreement with the XRD data. This indisputably confirms the enhanced tendency of sample 10-98 to generate crystal domains, probably due to the synergistic effect of both a high hydrolysis degree and a low molecular weight.

The huge difference in thermal properties between the low DH samples (4-88 and 40-88) and the sample 10-98 gives reason for the observed release patterns. It is well established that the region of the polymer in which water molecules can be taken up is only the amorphous phase of PVOH. As a consequence of water absorption, the mobility of the polymer chains in the amorphous region will increase, with a concomitant shift of the T_g towards lower temperatures due to the plasticizing effect of water [47,58], which causes the polymer to undergo a glass to rubber transition [59]. Lowering of the T_g results in the relaxation of the network chains, which is macroscopically accompanied by the swelling of the matrix. As mentioned before, this is restrained by high degree of crystallinity, as in the case of sample 10-98. Therefore, it can be said that the lower amount of dye released from sample 10-98 must be related to the decreased diffusion of the penetrant (water) and the decreased relaxation of the polymer chains compared to samples 40-88 and 4-88, which in turn exhibited an increased swelling behavior.

3.4. Films morphology

Samples of similar thickness, weight and dry matter (Table 1) were used to obtain the cross-section SEM images at two different magnifications (20k× and 40k×) shown in Figure 6, which highlight the global morphology of the polymer network. Sample 4-88 exhibited a spiky "stalactite-like" morphology (20k× magnification), with an apparently high degree of interstices and empty spaces within the molecular chain network (40k× magnification). The overall morphology changed dramatically for the sample 40-88, i.e. with increased molecular weight. This sample showed an apparently rougher morphology, with an "orange peel-like" texture (20k× magnification) due to

molecular aggregates seemingly oriented parallel to the longitudinal direction (40k× magnification). Finally, sample 10-98 displayed a more compact and tighter structure (20k× magnification), presumably with very limited free volume between polymer chains (40k× magnification).

Although SEM images cannot provide direct information on molecular mechanisms, the different morphologies observed for the three PVOH samples can be tentatively linked to the physicochemical heterogeneity of the polymer matrices, i.e. in terms of molecular weight and degree of hydrolysis. On one hand, apparently aggregated morphologies (e.g. sample 40-88) can be due to extensive molecular folding and entanglements, which are well known to increase proportionally with the molecular weight. On the other hand, denser structures (e.g. sample 10-98) are probably induced by higher degree of hydrolysis because of the increased intramolecular and intermolecular cohesive energy of the polymer, mainly driven by extensive hydrogen bonding between the hydroxyl groups along the polymer backbone. At the same time, the low molecular weight of sample 10-98 might have promoted the establishment of intermolecular hydrogen bonds due to high chain mobility. These considerations are in agreement with both the XRD and DSC data previously discussed. In particular, the structural change from the packed lamellar structure of sample 10-98 to the fibril-like and disordered structures of samples 40-88 and 4-88, respectively, appeared to be linked to broadening of the XRD peak area, which involves a depression of crystallinity.

Observations arising from the SEM analysis suggest that the release profile of the molecule dye from the PVOH matrices can be somehow influenced by different morphologies (presumably linked to different molecular arrangements), which in turn can be induced by a proper selection of the polymer matrix.

3.5. Effect of the solvent composition

The effect of the hydro-alcoholic solution in contact with the PVOH matrices cannot be neglected in the discussion of the aforementioned results. Mixing water with another solvent at various ratios is a well-established practice to modulate the solubility of hydrophilic polymers such as PVOH. In particular, with respect to the development of controlled release systems, the solvent composition becomes an important factor to control the swelling behavior of the polymer. The water/ethanol mixing ratio used in this work (1/9) allowed monitoring the release of the dye from all the three PVOH films, without dissolution of the films being observed over the entire duration of the experiments. The same results would have been otherwise unattainable with both ethanol richer solutions and water richer solution, due to a too low and too high relaxation of the polymer matrix, respectively. In other words, the presence of ethanol in the mixture made possible to tune the release rate by controlling the relaxation of the polymer chains to the extent that both fast relaxation and very slow relaxation were avoided. This is thought to be due to the different local affinity of the two solvents towards PVOH, the water molecules having higher affinity. Therefore, it can be said that ethanol somehow counterbalanced the effect of water molecules on the PVOH physical properties, e.g. ethanol hindered crystallites dissolution and other macroscopic phenomena such as crazing, waving and abrupt increase of swelling followed by catastrophic expansion of the swollen film, which are typical of water-rich solvents.

4. Conclusions

In this work, the different release kinetics of a small molecule (Coomassie blue dye) from three different PVOH films into a hydro-alcoholic solution were investigated over an extended temporal window (one month). Our results showed that the release from PVOH is mainly controlled by its chemical composition, i.e. the degree of substitution of the acetate groups by hydroxyl groups, which in turn dictates the degree of crystallinity, as unequivocally demonstrated by diffraction, thermal, and

morphological analyses. The crystallinity played an important role in controlling the release properties of the PVOH matrices insomuch as the final release system can be reasonably considered as a crystal dissolution-controlled system. Molecular weight was shown to affect the overall release properties to a less extent. Apparently, higher level of molecular chain entanglement hindered the mobility of the entrapped molecule through the molecular polymer chains. The use of ethanol also influenced the ultimate release properties of the three PVOH samples. Due to its non-solvent feature toward this polymer, ethanol made possible avoiding both abrupt volumetric expansion and complete dissolution of the matrices over the entire time of analysis. Finally, the affinity between the polymer matrix and the loaded molecule could have promoted the establishment of new weak intermolecular forces, e.g. ion-dipole interactions, which would have somehow affected the final amount of the dye released. These results, together with the mathematical modeling of the release kinetics, can be profitably used for the development of delivery systems for different applications, where the controlled release over time of an active molecule is the target.

Acknowledgements

We are thankful to Dr. F. Demartin and Dr L. Introzzi (University of Milan) for technical and scientific assistance.

References

[1] S. Wu, F. Li, H. Wang, L. Fu, B. Zhang, G. Li, Effects of poly (vinyl alcohol) (PVA) content on preparation of novel thiol-functionalized mesoporous PVA/SiO2 composite nanofiber membranes and their application for adsorption of heavy metal ions from aqueous solution, Polymer 51 (2010) 6203–6211.

[2] J.H. Sung, M.-R. Hwang, J.O. Kim, J.H. Lee, Y.I. Kim, J.H. Kim, S.W. Chang, S.G. Jin, J.A. Kim, W.S. Won Lyoo, S.S. Han, S.K. Ku, C.S. Yong, H.-G. Choi, Gel characterisation and in vivo evaluation of minocycline-loaded wound dressing with enhanced wound healing using polyvinyl alcohol and chitosan, Int. J. Pharm. 392 (2010) 232–240.

[3] A.S. Asran, S. Henning, G.H. Michler. Polyvinyl alcohol–collagen–hydroxyapatite biocomposite nanofibrous scaffold: Mimicking the key features of natural bone at the nanoscale level, Polymer 51 (2010) 868–876.

[4] N. De Prisco, B. Immirzi, M. Malinconico, P. Mormile, L. Petti, G. Gatta, Preparation, physico-chemical characterization, and optical analysis of polyvinyl alcohol-based films suitable for protected cultivation, J. Appl. Polym. Sci. 86 (2002) 622–632.

[5] I.-G. Marino, P.P. Lottici, C. Razzetti, A. Montenero, M. Rocchetti, M. Toselli, M. Marini, F. Pilati, Polariscopic imaging and vibrational characterization of hybrid films for packaging, Packag. Technol. Sci. 21 (2008) 329–338.

[6] S. Yun, H. Im, Y. Heo, J. Kim, Crosslinked sulfonated poly(vinyl alcohol)/sulfonated multi-walled carbon nanotubes nanocomposite membranes for direct methanol fuel cells, J. Membrane Sci. 380 (2011) 208–215.

[7] M.S. Boroglu, S.U. Celik, A. Bozkurt, I. Boz, The synthesis and characterization of anhydrous proton conducting membranes based on sulfonated poly(vinyl alcohol) and imidazole, J. Membrane Sci. 375 (2011) 157–164.

[8] R. Nirmala, D. Kalpana, J.W. Jeong, H.J. Oh, J.-H. Lee, R. Navamathavan, Y.S. Lee, H.Y. Kim, Multifunctional baicalein blended poly(vinyl alcohol) composite nanofibers via electrospinning, Colloids Surf. A 384 (2011) 605–611.

[9] J.-S. Park, J.-W. Park, E. Ruckenstein, Thermal and dynamic mechanical analysis of PVA/MC blend hydrogels, Polymer 42 (2001) 4271–4280.

[10] S. Liang, Q. Huang, L. Liu, K.L. Yam, Microstructure and molecular interaction in glycerol plasticized chitosan/poly(vinyl alcohol) blending films, Macromol. Chem. Phys. 210 (2009) 832–839.

[11] E. Chiellini, P. Cinelli, V.I. Ilieva, M. Martera, Biodegradable thermoplastic composites based on polyvinyl alcohol and algae, Biomacromolecules 9 (2008) 1007–1013.

[12] S.R. Sudhamani, M.S. Prasad, K.U. Sankar, DSC and FTIR studies on gellan and polyvinyl alcohol (PVA) blend films, Food Hydrocolloid. 17 (2003) 245–250.

[13] R.M. Dicharry, P. Ye, G. Saha, E. Waxman, A.D. Asandei, R.S. Parnas, Wheat gluten−thiolated poly(vinyl alcohol) blends with improved mechanical properties, Biomacromolecules 7 (2006) 2837–2844.

[14] M. Kobayashi, J. Toguchida, M. Oka, Preliminary study of polyvinyl alcohol-hydrogel (PVA-H) artificial meniscus, Biomaterials 24 (2003) 639–647.

[15] M. Moreno, R. Hernández, D. López, Crosslinking of poly(vinyl alcohol) using functionalized gold nanoparticles, Eur. Polym. J. 46 (2010) 2099–2104.

[16] P.W. Labuschagne, W.A. Germishuizen, S.M.C. Verryn, F.S. Moolman, Improved oxygen barrier performance of poly(vinyl alcohol) films through hydrogen bond complex with poly(methyl vinyl ether-co-maleic acid), Eur. Polym. J. 44 (2008) 2146–2152.

[17] S.A. Poursamar, M. Azami, M. Mozafari, Controllable synthesis and characterization of porous polyvinyl alcohol/hydroxyapatite nanocomposite scaffolds via an in situ colloidal technique, Colloids Surf. B 84 (2011) 310–316.

[18] D.L. Kaplan, J.M. Mayer, D. Ball, J. McCassie, S. Stenhouse, Fundamentals of Biodegradable Polymers, in: C. Ching, D.L. Kaplan, E.L. Thomas (Eds.), Biodegradable Polymers and Packaging, Technomic Publishing Inc, Lancaster, 1993, p. 152.

[19] I. Moreno, V. González-González, J. Romero-García, Control release of lactate dehydrogenase encapsulated in poly (vinyl alcohol) nanofibers via electrospinning, Eur. Polym. J. 47 (2011) 1264–1272.

[20] J.K. Li, N. Wang, X.S. Wu, Poly(vinyl alcohol) nanoparticles prepared by freezing–thawing process for protein/peptide drug delivery, J. Control. Release 56 (1998) 117–126.

[21] F. Schwenter, N. Bouche, W.-F. Pralong, P. Aebischer, In vivo calcium deposition on polyvinyl alcohol matrix used in hollow fiber cell macroencapsulation devices, Biomaterials 25 (2004) 3861–3868.

[22] X. Jin, Y.-L. Hsieh, pH-responsive swelling behavior of poly(vinyl alcohol)/poly(acrylic acid) bi-component fibrous hydrogel membranes, Polymer 46 (2005) 5149–5160.

[23] K. Juntanon, S. Niamlang, R. Rujiravanit, A. Sirivat, Electrically controlled release of sulfosalicylic acid from crosslinked poly(vinyl alcohol) hydrogel, Int. J. Pharm. 356 (2008) 1–11.

[24] S.M. Shaheen, K. Yamaura, Preparation of theophylline hydrogels of atactic poly(vinyl alcohol)/NaCl/H2O system for drug delivery system, J. Control. Release 81 (2002) 367–377.

[25] J. Huang, H. Kao, X.Y. Wu, The pH-dependent biphasic release of azidothymidine from a layered composite of PVA disks and P(MMA/MAA) spheres, J. Control. Release 67 (2000) 45–54.

[26] D. Dainelli, N. Gontard, D. Spyropoulos, E. Zondervan-van den Beukend, P. Tobback, Active and intelligent food packaging: legal aspects and safety concerns, Trends Food Sci. Tech. 19 S1 (2008) 103–112.

[27] H.-B. Liu, Q. Yan, C. Wang, X. Liu, C. Wang, X.-H. Zhou, S.-J. Xiao, Saccharide- and temperature-responsive polymer brushes grown on gold nanoshells for controlled release of diols, Colloids Surf. A 386 (2011) 131–134.

[28] K.-W. Yeh, C.P. Chang, T. Yamamoto, T. Dobashi, Release model of alginate microcapsules containing volatile tea-tree oil, Colloids Surf. A 380 (2011) 152–155.

[29] S.K. Klee, M. Farwick, P. Lersch, Triggered release of sensitive active ingredients upon response to the skin's natural pH, Colloids Surf. A 338 (2009) 162–166.

[30] D. Costa, A.J.M. Valente, M.G. Miguel, B. Lindman, Light triggered release of solutes from covalent DNA gels, Colloids Surf. A 391 (2011) 80–87.

[31] E.F. Small, M.C. Willy, P.A. Lewin, S.P. Wrenn, Ultrasound-induced transport across lipid bilayers: Influence of phase behavior, Colloids Surf. A 390 (2011) 40–47.

[32] J. Yun, J. S. Im, Y.-S. Lee, T.-S. Bae, Y.-M. Lim, H.-I. Kim, pH and electro-responsive release behavior of MWCNT/PVA/PAAc composite microcapsules, Colloids Surf. A 368 (2010) 23–30.

[33] K. Pal, A.K. Banthia, D.K. Majumdar, Preparation and characterization of polyvinyl alcohol-gelatin hydrogel membranes for biomedical applications, AAPS PharmSciTech. 8 (2007) 142–146.

[34] G.G. Buonocore, M.A. Del Nobile, A. Panizza, S. Bove, G. Battaglia, L. Nicolais, Modeling the lysozyme release kinetics from antimicrobial films intended for food packaging applications, J. Food Sci. 68 (2003) 1365–1370.

[35] G.G. Buonocore, M.A. Del Nobile, A. Panizza, M.R. Corbo, L. Nicolais, A general approach to describe the antimicrobial agent release from highly swellable films intended for food packaging applications, J. Control. Release 90 (2003) 97–107.

[36] Commission Regulation (EU) No 10/2011 of 14 January 2011 on plastic materials and articles intended to come into contact with food. Official Journal of the European Union, L 12/1–L 12/89.

[37] G.E. Ward, K.L. Carey, N.J. Westwood, Using small molecules to study big questions in cellular microbiology, Cell. Microbiol. 4 (2002) 471–482.

[38] H.J. Chial, H.B. Thompson, A.G. Splittgerber, A spectral study of the charge forms of coomassie blue G, Anal. Biochem. 209 (1993) 258–266.

[39] O. Fuchs, Polymer Handbook, third ed., John Wiley and Sons, New York, 1989.

[40] N. Peppas, E. Merrill, Differential scanning calorimetry of crystallized PVA hydrogels, J. Appl. Polym. Sci. 20 (1976) 1457–1465.

[41] M. Mastromatteo, G. Barbuzzi, A. Conte, M.A. Del Nobile, Controlled release of thymol from zein based film, Innov. Food Sci. Emerg. 10 (2009) 222–227.

[42] R. Langer, N. Peppas, Chemical and physical structure of polymers as carriers for controlled release of bioactive agents: a review. Macromol. Chem. Physic. C23 (1983) 61–126.

[43] J. Crank, The mathematics of diffusion, Clarendon Press, Oxford, 1975.

[44] R. Morita, R. Honda, Y. Takahashi, Development of oral controlled release preparations, a PVA swelling controlled release system (SCRS) I. Design of SCRS and its release controlling factor, J. Control. Release 63 (2000), 297–304.

[45] C.W. Bunn, Crystal structure of polyvinyl alcohol, Nature 161 (1948) 929–930.

[46] G.M. Kim, A.S. Asran, G.H. Michler, P. Simon, J.S. Kim, Electrospun PVA/HAp nanocomposite nanofibers: biomimetics of mineralized hard tissues at a lower level of complexity, Bioinspir. Biomim. 3 (2008) 1–12.

[47] H.E. Assender, A.H. Windle, Crystallinity in poly(vinyl alcohol). 1. An X-ray diffraction study of atactic PVOH, Polymer 39 (1998) 4295–4302.

[48] U.W. Gedde, Polymer Physics, Kluwer Academic Publishers, Dordrecht, 1995.

[49] L.M. Döppers, C. Breen, C. Sammon, Diffusion of water and acetone into poly(vinyl alcohol)–clay nanocomposites using ATR-FTIR, Vib. Spectrosc. 35 (2004) 27–32.

[50] T. Tanigami, K. Yano, K. Yamaura, S. Matsuzawa, Anomalous swelling of poly(vinyl alcohol) film in mixed solvents of dimethylsulfoxide and water, Polymer 36 (1995) 2941–2946.

[51] S.K. Mallapragada, N.A. Peppas, Crystal dissolution-controlled release systems: I. Physical characteristics and modeling analysis, J. Control. Release 45 (1997) 87–94.

[52] C.M. Hassan, N.AA. Peppas, Structure and applications of poly(vinyl alcohol) hydrogels produced by conventional crosslinking or by freezing/thawing methods, Adv. Polym. Sci. 153 (2000) 37–65.

[53] I. Sakurada, Y. Nukushina, Y. Sone, Relation between crystallinity and swelling of poly(vinyl alcohol), Kobunshi Kagaku 12 (1955) 510–513.

[54] T.G. Fox, P.J. Flory, Second-order transition temperatures and related properties of polystyrene. I. Influence of molecular weight, J. Appl. Phys. 21 (1950) 581–591.

[55] F.L. Martien, Encyclopedia of Polymer Science and Engineering, John Wiley and Sons, New York, 1986.

[56] R.M. Hodge, G.H. Edward, G.P. Simon, Water absorption and states of water in semicrystalline poly(vinyl alcohol) films, Polymer 37 (1996) 1371–1376.

[57] R.M. Hodge, T.J. Bastow, G.H. Edward, G.P. Simon, A.J. Hill, Free Volume and the mechanism of plasticization in water-swollen poly(vinyl alcohol), Macromolecules 29 (1996) 8137–8143.

[58] C.A. Finch, Poly(vinyl alcohol): properties and applications, John Wiley and Sons, New York, 1973.

[59] N.L. Thomas, A. H. Windle, A deformation model for Case II diffusion, Polymer 21 (1980) 613–619.

Figure captions

Figure 1. Chemical structure of the Coomassie Brilliant Blue G dye used in this work as the model drug-like compound for the release study.

Figure 2. Original (a) and back-shifted experimental (symbols) and calculated (line) release data (b) of the Coomassie brilliant blue dye at 20°C from the 4-88 (□), 40-88 (△), and 10-98 (◇) PVOH film samples. Samples as appeared after 33 days immersion in the water/ethanol solution (c).

Figure 3. Swelling ratio evolution of PVOH samples 4-88 (□), 40-88 (△), and 10-98 (◇) during the first 24 hours of the release experiment and after 13 days (b).

Figure 4. XRD traces of the 4-88 (—), 40-88 (—), and 10-98 (—) PVOH films.

Figure 5. Representative DSC traces (second heating scan) of the 4-88 (□), 40-88 (△), and 10-98 (◇) dried PVOH samples.

Figure 6. Cross-sectional SEM images (20k×, left column; 40k×, right column) of the three PVOH films. Images in the same row are from the same sample.

Table 1

Table 1. Dry weight, moisture content, thickness (l), partition coefficient PVOH/solvent (K), and diffusion coefficients (D_1 and D_2) of the dye-loaded PVOH films.

PVOH type	Dry weight (g)	Moisture content (%)	l (μm)	K	D_1 (cm^2/s)	D_2 (cm^2/s)
4-88	$0.27^{a} \pm 0.011$	$1.80^{cd} \pm 0.52$	$63.75^{ef} \pm 6.28$	0.68 ± 0.08^{g}	$8.33E\text{-}11^{l}$	$2.50E\text{-}11^{n}$
40-88	$0.26^{b} \pm 0.004$	$1.12^{c} \pm 0.41$	$64.17^{e} \pm 0.88$	1.24 ± 0.14^{h}	$8.33E\text{-}11^{l}$	$5.83E\text{-}12^{o}$
10-98	$0.26^{ab} \pm 0.002$	$1.93^{d} \pm 0.41$	$56.33^{f} \pm 5.01$	9.95 ± 0.96^{i}	$1.16E\text{-}11^{m}$	$2.00E\text{-}11^{n}$

Different superscripts within a group (i.e. within each parameter) denote a statistically significant difference ($p < 0.05$).

Table 2. Main parameters obtained from the XRD traces of the different PVOH films.

PVOH type	Diffraction peak (2θ)	Peak intensity	Peak area	Crystallite size (nm)
4-88	19.68	1000	4727.61	2.30
40-88	19.20	1000	2802.89	3.53
10-98	19.06	869.24	1656.35	4.04

Table 3. Glass transition temperature (T_g), melting temperature (T_m), and crystallinity degree (x_c) obtained from the DSC traces of the different PVOH films.

PVOH type	T_g (°C)	T_m (°C)	x_c (%)
4-88	60.14 (± 0.54)[a]	170.21 (± 1.35)[c]	15.98 (± 1.24)[e]
40-88	66.94 (± 3.38)[b]	168.12 (± 2.51)[c]	13.62 (± 1.71)[e]
10-98	71.77 (± 3.43)[b]	219.55 (± 0.75)[d]	50.96(± 2.13)[f]

Different superscripts within a group (i.e. within each parameter) denote a statistically significant difference ($p < 0.05$).

Figure 1

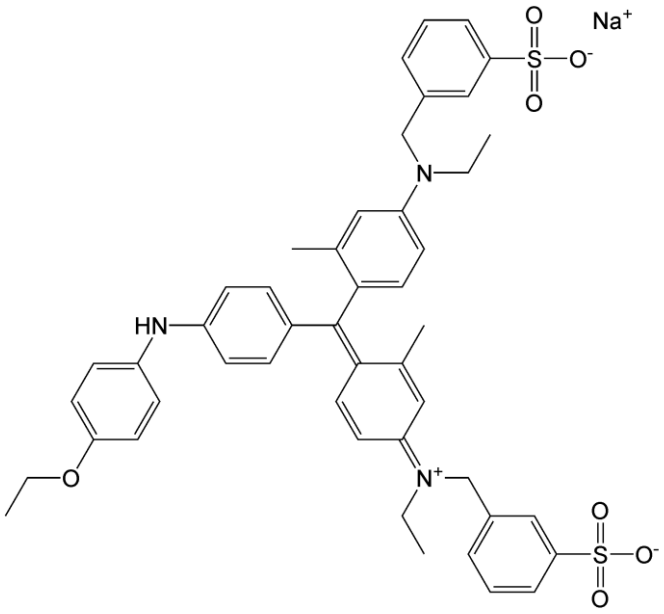

Figure 1. Chemical structure of the Coomassie Brilliant Blue G dye used in this work as the model drug-like compound for the release study.

Figure 2

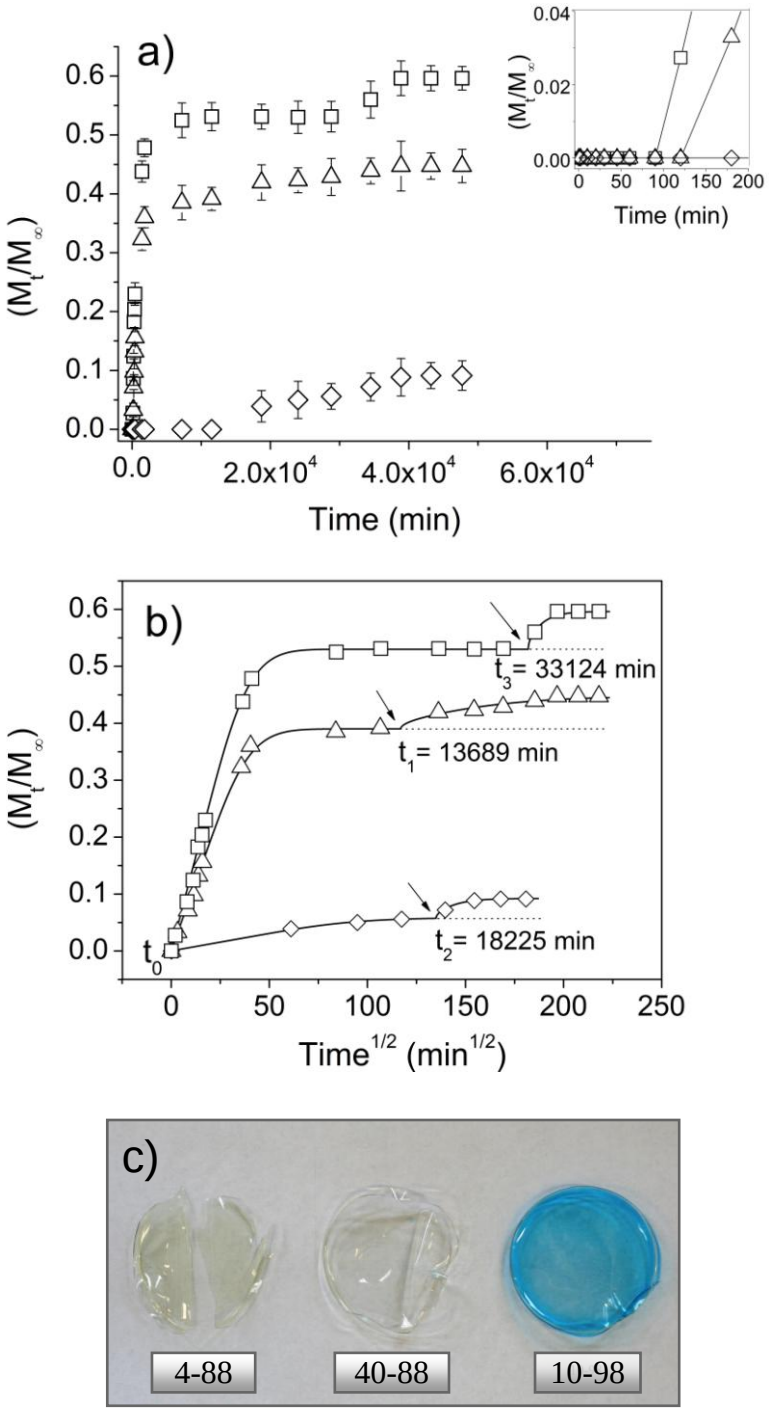

Figure 2. Original (a) and back-shifted experimental (symbols) and calculated (line) release data (b) of the Coomassie brilliant blue dye at 20°C from the 4-88 (□), 40-88 (△), and 10-98 (◇) PVOH film samples. Samples as appeared after 33 days immersion in the water/ethanol solution (c).

Figure 3

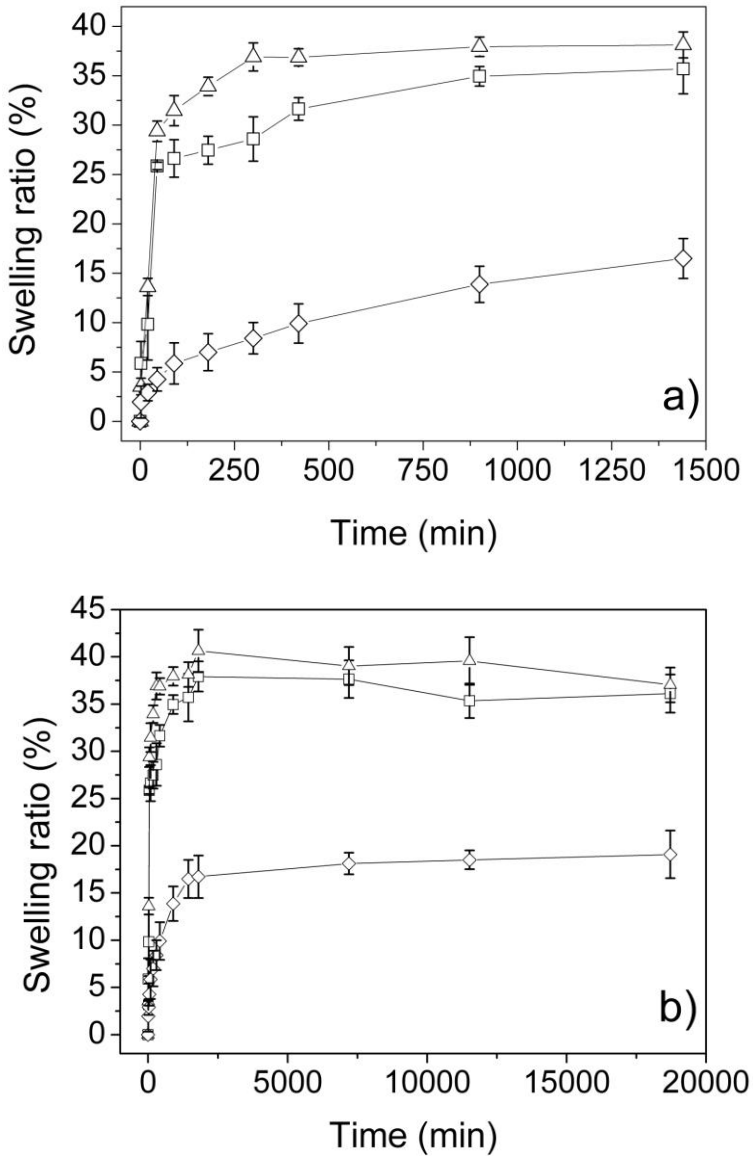

Figure 3. Swelling ratio evolution of PVOH samples 4-88 (□), 40-88 (△), and 10-98 (◇) during the first 24 hours of the release experiment (a) and after 13 days (b).

Figure 4

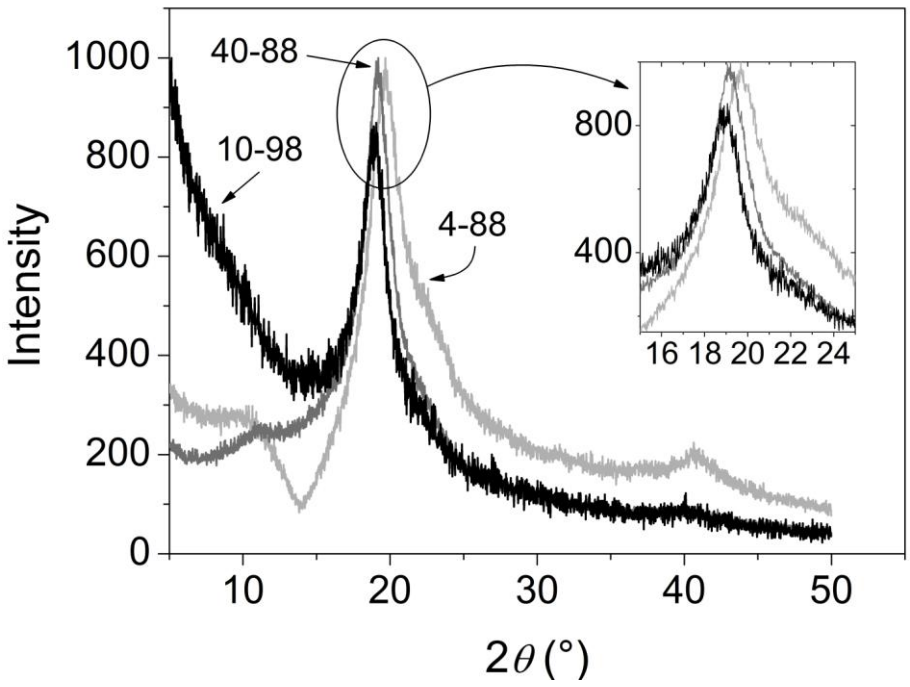

Figure 4. XRD traces of the 4-88 (—), 40-88 (—), and 10-98 (—) PVOH films.

Figure 5

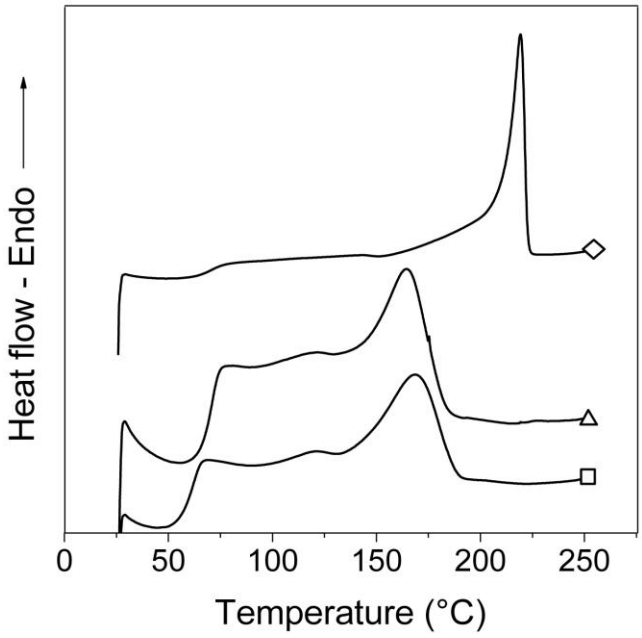

Figure 5. Representative DSC traces (second heating scan) of the 4-88 (□), 40-88 (△), and 10-98 (◇) dried PVOH samples.

Figure 6

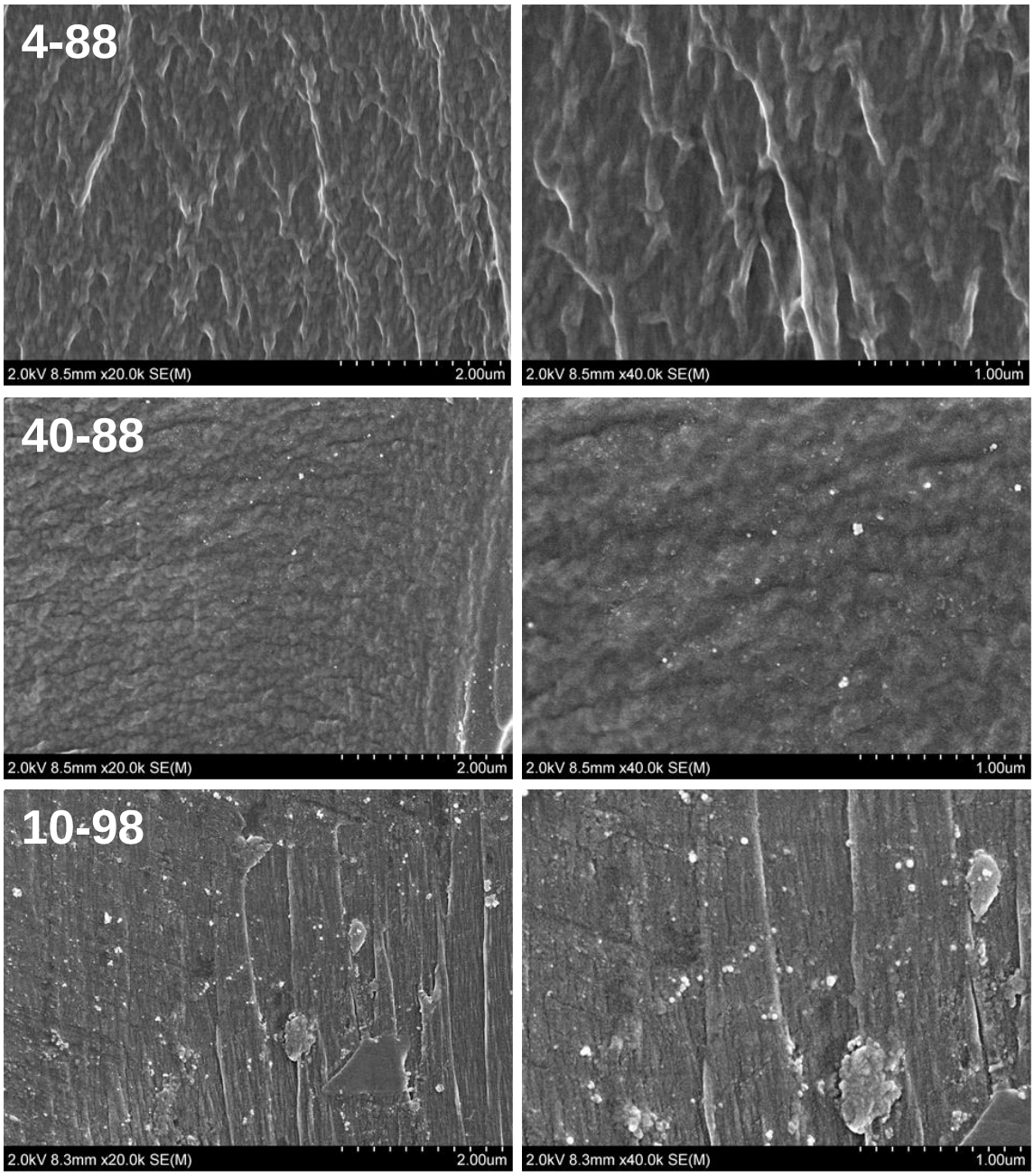

Figure 6. Cross-sectional SEM images (20k×, left column; 40k×, right column) of the three PVOH films. Images in the same row are from the same sample.